Available online at www.sciencedirect.com
ScienceDirect
Journal of the European Ceramic Society 29 (2009) 3409–3417
www.elsevier.com/locate/jeurceramsoc

Thermal properties of the nitrogen-rich Ca-α-Sialons

Yanbing Cai *, Mats Nygren, Zhijian Shen, Jekabs Grins, Saeid Esmailzadeh

Department of Physical, Inorganic and Structural Chemistry, Arrhenius Laboratory, Stockholm University, SE-10691 Stockholm, Sweden

Received 4 November 2008; received in revised form 4 June 2009; accepted 15 July 2009
Available online 8 August 2009

Abstract

Nitrogen-rich Ca-α-Sialon ($Ca_xSi_{12-2x}Al_{2x}N_{16}$ with $x = 0.2$, 0.4, and 0.8, 1.2 and 1.6) ceramics were prepared from the mixtures of Si_3N_4, AlN and CaH_2 powders in a hot press at 1800 °C using a pressure of 35 MPa and a holding time of 4 h, and then were investigated with respect to reaction mechanism, phase stability and oxidation resistance. In addition the sample with $x = 1.6$ was prepared in the temperature range 600–1800 °C using a pressure of 35 MPa and a holding time of 2 h. The α-Sialon phase was first observed at 1400 °C but the α-Si_3N_4 and AlN phases were still present at 1700 °C. Phase pure Ca-α-Sialon ceramics could not be obtained until the sintering temperature reached 1800 °C. The phase pure nitrogen-rich Ca-α-Sialon exhibited no phase transformation in the temperature range 1400–1600 °C. In general, mixed α/β-Sialon showed better oxidation resistance than pure α-Sialon in the low temperature range (1250–1325 °C), while α-Sialons with compositions located at α/β-Sialon border-line showed significant weight gains over the entire temperature range tested (1250–1400 °C). The phases formed upon oxidation were characterized by X-ray, SEM and TEM studies.

Keywords: Sialon; Si_3N_4; Hot pressing; Thermal properties; Nitrogen rich

1. Introduction

α-Sialon is a solid solution of α-Si_3N_4 that can be expressed as $M_xSi_{12-(m+n)}Al_{m+n}O_nN_{16-n}$, where M = Li, Mg, Ca, Y and most lanthanide elements. In general, α-Sialon ceramics have been considered to be hard materials however as in many cases α-Sialon ceramics contain equi-axed grains, these α-Sialons possess inferior fracture toughness relative to β-Sialon ($Si_{6-z}Al_zO_zN_{8-z}$, with $0 < z < 4.2$) ones.[1,2] Si_3N_4-based ceramics, mainly find their applications in cutting tools, ceramics ball-bearings and rollers or other applications that require a combination of high toughness and (hot) hardness. These properties are strongly determined by the obtained microstructures, phase compositions and the chemistry of intergranular grain boundary glass phase. It has been shown that nitrogen-rich Ca-α-Sialons ($Ca_xSi_{12-2x}Al_{2x}N_{16}$) ceramics can be prepared from the mixtures of Si_3N_4, AlN and CaH_2 powders.[3] Based on the positive effects of increasing nitrogen content vis-a-vis the properties of the formed oxynitride glass with respect to glass transition temperature, hardness, toughness, etc., CaH_2 has been used as Ca source in stead of CaO that traditionally has been used in connection with the preparation of Ca-α-Sialons. The nitrogen-rich Sialons, that theoretically have compositions that can be expressed as $M_xSi_{12-vx}Al_{vx}O_nN_{16}$, where v denotes the valence of M cations, have not been studied in greater detail mainly due to the difficulties associated with the handling of moisture sensitive metal nitrides. The present work deals with the preparation of some nitrogen-rich Ca-α-Sialon ($Ca_xSi_{12-2x}Al_{2x}N_{16}$) ceramics that exhibit improved toughness that in turn can be attributed to the formation of elongated α-Sialon grains.[3,4] In addition, increased resistance to high temperature deformation was also observed in nitrogen-rich Ca-α-Sialons, i.e. nitrogen-rich Ca-α-Sialons exhibited about 150 °C higher deformation onset temperature than those of their oxygen-rich counterparts.[5] In the present study, thermal properties of nitrogen-rich Ca-α-Sialons are investigated with respect to reaction mechanism, phase stability and oxidation resistance with the aim to elucidate their high temperature properties.

2. Experimental

Details about sample preparation can be found in Ref. 3. In brief, mixtures of the starting powders of Si_3N_4 (UBE SN-E10), AlN (Tokuyama, grade F), and CaH_2 (Alfa Aesar Johnson

* Corresponding author. Tel.: +46 8 163081; fax: +46 8 152187.
E-mail address: yanbingcai@gmail.com (Y. Cai).

0955-2219/$ – see front matter © 2009 Elsevier Ltd. All rights reserved.
doi:10.1016/j.jeurceramsoc.2009.07.015

Matthey Chemicals Ltd) according to the nominal composition of $Ca_xSi_{12-2x}Al_{2x}N_{16}$, with $x = 0.2$, 0.4, and 0.8, 1.2 and 1.6, respectively, were ball milled (planetary ball mill PM 100, Retsch, Germany) in hexane and these samples are denoted as CCH02, CCH04, CCH08, CCH12, and CCH16. The mixed powders were vacuum-dried at 105 °C for 6 h then pre-compacted in a steel die in an argon-filled glove box, and finally hot pressed using a pressure of 35 MPa and a holding time of 4 h at 1800 °C. In order to reveal the reaction subsequences, starting powders of CCH16 composition were hot pressed in the temperature range 600–1800 °C for 2 h using a pressure of 35 MPa, followed by an X-ray powder diffraction analysis. For the same composition, thermal gravity analysis was also carried out in a TG unit (SETARAM TAG 24, Setaram, France) using a heating rate of 10 °C/min in nitrogen atmosphere, with a purpose of monitoring the decomposition and nitridation processes supposed to happen with increasing temperature up to 1200 °C. Oxidation experiments were performed in the same TG unit at 1250 °C, 1325 °C and 1400 °C. The samples were heated to these temperatures with a heating rate of 10 °C/min and the duration of the oxidation experiment was 20 h in flowing oxygen. Prior to oxidation, samples of the approximate size of 10 mm × 3 mm × 1 mm were cut, ground, and polished with diamond suspensions down to 1 μm. The samples were connected to the hang down wire of the TG-unit via a notch with depth of 1 mm that was made at the end of sample bars by using a 0.5-mm thick diamond blade. The drift of the set-up was corrected via recording time versus weight loss curves of Al_2O_3 dummies at 1250 °C, 1325 °C and 1400 °C.

Phase assemblages of samples before and after heat treatment at different temperatures were identified by their X-ray powder diffraction patterns recorded in a Guinier-Hägg focusing camera with 50 mm radius using Cu $K\alpha_1$ radiation. Si was used as the internal standard. The phases present in the oxide scales were identified by their X-ray powder diffraction patterns recorded in a D/Max-2250 V diffractometer (Rigaku, Tokyo, Japan) operated in reflection mode, using Cu $K\alpha_1$ radiation.

The microstructures were recorded in a scanning electron microscopy (SEM; JEOL JSM-7000F, Tokyo, Japan) equipped with an energy dispersive spectrometry (EDS; Link Isis, Oxford Instruments, Buckinghamshire, UK). A back scattered electron (BSE) mode and accelerating voltage of 10 kV were used, so as to reduce the electron interaction volumes. Prior to SEM investigation, the polished surfaces of the samples were etched in a molten mixture of KOH and KNO_3 for 1–3 min before carbon coating. Transmission electron microscopy (TEM) and high resolution transmission electron microscope (HRTEM) observations were carried on JEOL JEM-3010 operated at 300 kV (Cs = 0.6 mm, resolution 1.7 Å). Images were recorded with a CCD camera (MultiScan model 794, Gatan, 1024 × 1024 pixel, pixel size 24 μm × 24 μm) under low-dose conditions.

3. Results and discussion

3.1. Phase analysis

The overall starting compositions and the phase assemblages found in the sintered samples are listed in Table 1. The prepared samples still contain a small amount of oxygen because that the starting powders Si_3N_4 and AlN contain some surface oxides. Dual phase α/β-Sialons are formed for $x = 0.2$ and 0.4, while single phase α-Sialons are obtained when $x = 0.8$, 1.2 and 1.6. There is no observation of secondary grain boundary crystalline phases, like AlN polytypes or gehlenite ($Ca_2Al_2SiO_7$) that were usually observed when CaO was used as a sintering additive.[6]

3.2. Microstructures of the sintered samples

The microstructures of the hot pressed samples are shown in Fig. 1. All samples but CCH04 contain elongated Sialon grains. The sample CCH04 exhibits a finer grained microstructure with almost equiaxed grains (Fig. 1b). When the starting composition is in the dual α/β-Sialon formation region, the elongated grains are β-Sialon phase, which usually develop into morphology with high aspect ratio (seen in CCH02). However, when the starting composition is in the α-Sialon formation region and is sintered at the same temperature, the development of elongated α-Sialon grains, especially in the case of Ca-α-Sialon, is dependent on the amount of transient liquid phase, which increases with increasing Ca^{2+} content. For sample CCH04, which has a composition locates at the border between dual-phase α/β-Sialon and single-phase α-Sialon, the amount of transient liquid phase formed is small and is then quickly consumed by the precipitation of α-Sialon grains, resulting in a glass-free ceramic with equal-axed grains.

With increasing CaH_2 content, a nitrogen saturated liquid with Ca^{2+} cations as glass network modifier kinetically facilitates the development of elongated Ca-α-Sialon grains. Well before the dissolution of Si_3N_4 and AlN at high temperatures, an oxynitride liquid Ca_3N_2–Al_2O_3–SiO_2 may form, rather than

Table 1
Overall starting compositions and crystalline phases found in the samples hot pressed at 1800 °C.

Sample	Compositions[a]	Powder mixture, wt%			Phases, mol%	
		CaH_2	Si_3N_4	AlN	α-Sialon	β-Sialon
CCH02	$Ca_{0.2}Si_{11.6}Al_{0.4}N_{15.53}O_{0.7}$	1.47	95.64	2.88	62	38
CCH04	$Ca_{0.4}Si_{11.2}Al_{0.8}N_{15.54}O_{0.69}$	2.91	91.38	5.71	97	3
CCH08	$Ca_{0.8}Si_{10.4}Al_{1.6}N_{15.55}O_{0.67}$	5.71	83.11	11.18	100	0
CCH12	$Ca_{1.2}Si_{9.6}Al_{2.4}N_{15.56}O_{0.66}$	8.39	75.18	16.44	100	0
CCH16	$Ca_{1.6}Si_{8.8}Al_{3.2}N_{15.57}O_{0.64}$	10.96	67.55	21.48	100	0

[a] The oxide contents in the starting powders are accounted for.

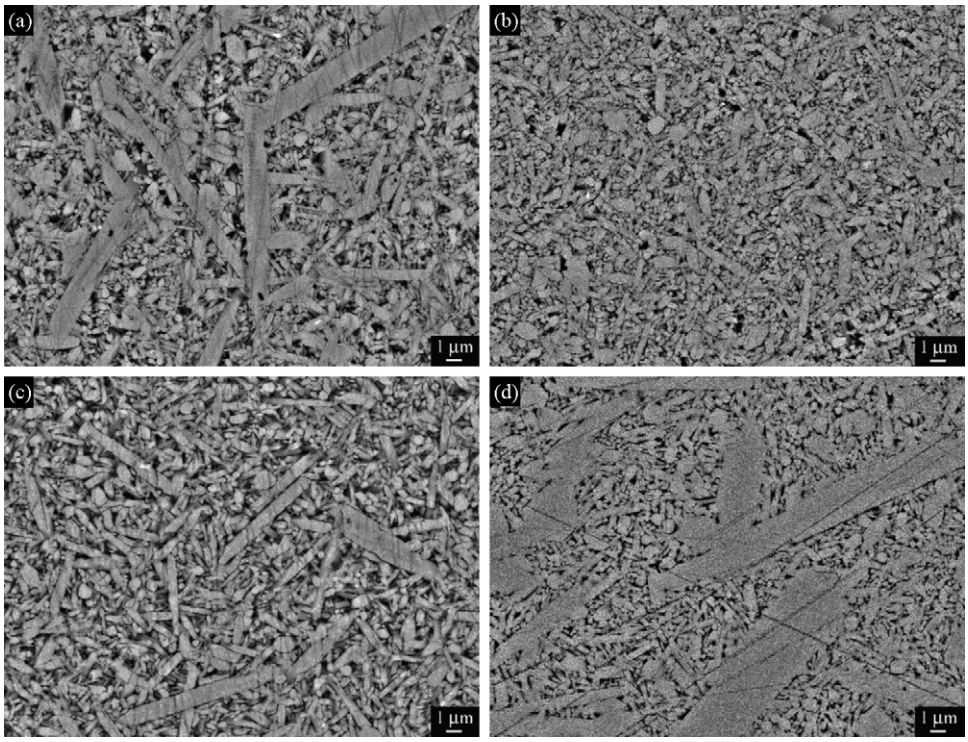

Fig. 1. SEM images of nitrogen-rich Ca-α-Sialons $Ca_xSi_{12-2x}Al_{2x}N_{16}$, (a) CCH02, (b) CCH04, (c) CCH08, and (d) CCH16.

an oxide liquid $CaO–Al_2O_3–SiO_2$ when using a CaO additive, in an amount increasing with increase in CaH_2 content. At higher temperatures, N, Si, and Al are introduced into the liquid by the dissolution of Si_3N_4 and AlN, and then consumed by the formation of the β-Sialon or α-Sialon phases. The pronounced growth along the *c* axis of α-Sialon grain can be attributed to changes of the Ca-α-Sialon grain surface energies induced by a nitrogen-rich calcium aluminum silicate glass. As indicated, the formation of α-Sialon is a solution-precipitation process that requires the presence of a liquid phase. The decomposition of CaH_2 is followed by an in situ formation of Ca_3N_2-containing phases that begins at a temperature around 300 °C and speeds up around 600 °C, as observed by TG and XRPD analysis (see below). The formation of the transient nitrides during the sintering process can be expected to increase the reactivity and to facilitate the formation of Sialon phase.

3.3. Reaction sequence and phase evolution

The TG-curve of ball-milled powders of the composition CCH16 recorded in N_2 atmosphere is shown in Fig. 2. Most of the weight loss occurred in the temperature region 200–300 °C, which is in agreement with the observed decomposition temperature of CaH_2 in various CaH_2 mixtures[7–9] while the decomposition temperature for pure CaH_2 is substantially higher (600 °C).[10] The weight loss is almost completed at 300 °C. The observed weight loss (0.38%) for CCH16 is less than the calculated one (0.53%), indicating that CaH_2 has partly decomposed in connection with the ball milling procedure and/or when the mixed powders were vacuum-dried, as mentioned above.

The TG curve of the sample CCH16 exhibits significant weight gain starting from 600 °C, and ended at $T > 800$ °C. Assuming that the weight gain can be ascribed to the reaction:

$$3Ca(s) + N_2(g) = Ca_3N_2(s) \quad (1)$$

The theoretical weight gain amounts to 1.9 wt% compared with the observed 1.5 wt%. The difference between observed and calculated weight gain can be ascribed to the observation that Ca also forms other compounds. Samples with CCH16 composition were hot pressed at temperatures ranging from 600 °C to

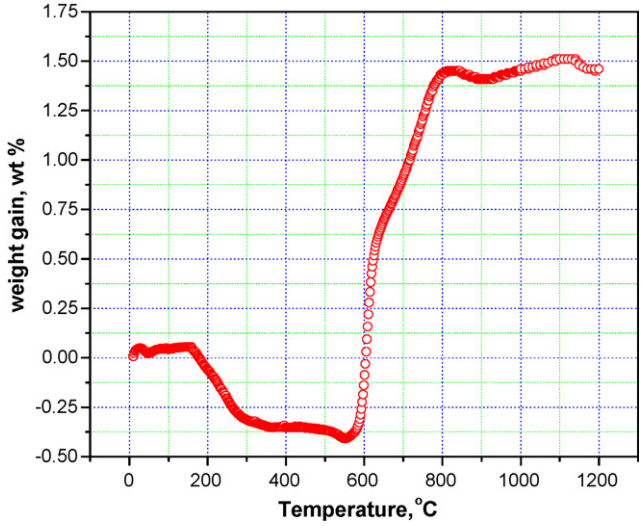

Fig. 2. TG curve of the powder mixture CCH16 recorded in flowing N_2. Weight loss occurs around 200 °C, and a significant weight gain is observed in temperature range 600–800 °C.

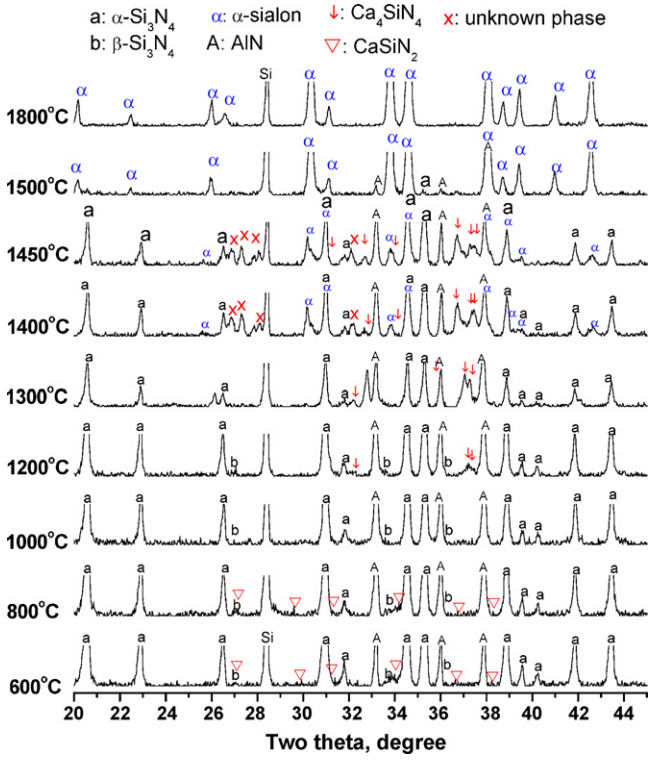

Fig. 3. XRPD patterns of the sample CCH16 hot pressed at different temperatures.

1800 °C under nitrogen atmosphere, and then were analyzed by the X-ray powder diffraction. As shown in Fig. 3, below 1450 °C, crystalline phases like $CaSiN_2$, Ca_4SiN_4 and an unknown transient phase are observed. As shown in the XRD patterns, the appearance of intermediate phases in sequence with increase of temperatures, together with the change of weight gain ratio observed at temperatures above 650 °C (see Fig. 2), indicates the formation of other intermediate phases, for example Ca_4SiN_4, directly through reaction of Ca, Si and N, or indirectly through reaction:

$$CaSiN_2(s) + 3Ca(s) + N_2(g) = Ca_4SiN_4(s) \quad (2)$$

The formation of calcium silicon nitrides is a quite complete process. The latter reaction (2), however, seems less possible under the present situation. First, CaH_2 powder has been further ground down into finer powder in the glove box and then homogeneously ball milled. This might be the reason that the observed decomposition temperature (200–300 °C) of CaH_2 in the TG analysis is significantly lower than that obtained from the literature (about 400 °C). Second, the decomposition of CaH_2 and consequently nitridation of Ca are assumed to happen at the same time, as there is no observation of characteristic peaks for Ca in the XRD patterns. Starting with a coarser CaH_2 powder, a certain amount of Ca metal might be left at relative low temperatures, then, at elevated temperatures, reacts with the previously formed $CaSiN_2$ to form the Ca_4SiN_4 phase. But this needs further identification under controlled conditions.

According to XRD patterns, the α-Sialon phase is observed at 1400 °C and the formation of α-Sialon from nitrogen-rich transient liquid via a solution-precipitation process is accelerated at 1500 °C, where only a small amount of the α-Si_3N_4 and AlN phases are present as secondary phases. These results are in agreement with the finding by Rutten et al.[11], i.e. they found that Ca-α-Sialon with a composition ($Ca_{0.8}Si_{9.6}Al_{2.4}O_{0.8}N_{15.2}$) is firstly formed at about 1350 °C and rapidly so at about 1450 °C. In contrary to our finding, Rutten et al. also observed the formation of intermediate phases like gehlenite ($CaAl_2SiO_7$) and/or AlN polytypiods. As mentioned above the monophasic Ca-α-Sialon ceramics were obtained at 1800 °C. The observation that the α-Sialon phase is firstly formed at 1400 °C in our case while Rutten et al. observed it already at 1350 °C can be ascribed to the low oxygen content in our powder mixture.

3.4. Thermal stability

It has been shown that the thermal stability of Ca-α-Sialons prepared with oxides additives is superior to the ones of rear earth stabilized Sialons[12,13] and so are rear earth stabilized Sialons co-doped with Ca.[14]

The thermal stability of the nitrogen-rich Ca-α-Sialons was studied as well. Hot pressed compacts of the compositions CCH02 (an α/β-Sialon), CCH04 (an α-Sialon containing traces of β-Sialon) and CCH16 (monophasic α-Sialon) were post heat treated in the temperature region 1400–1600 °C for 24 h. The X-ray powder diffraction patterns of the post heat treated samples are given in Fig. 4. Based on lattice calculation and diffraction patterns observation, it can be concluded that there is no significant difference between the X-ray powder diffraction patterns of the sintered and post heat treated samples, i.e. no α to β phase transformation takes place in these samples. In contrast, most α-Sialons stabilized by rear earth cations are prone to transform into β-Sialon and grain boundary phases in the temperature region 1300–1600 °C.[15–18] This finding, together with the findings by Hewett et al.[12] and Mandal and Thompson[13], that oxygen-rich Ca-α-Sialons are stable even when sintered with excess glass phase, indicates that calcium stabilized α-Sialons is probably the most thermal stable Sialon phase over a wide composition and temperature range. Low oxygen contents of starting compositions often yield less amounts of grain boundary glass phase in the sintered body, and the formed grain boundary phase has, due to its higher nitrogen content, higher viscosity than an oxygen-rich grain boundary phase. In the former case the α to β phase transformation is expected to be kinetically retarded.

Low and high resolution transmission electron microscopy studies focused on grain boundaries and triple-grain pockets provide us with some additional information about the glassy grain boundary phase. Thus direct bonding of grains is observed in sample CCH04, which has a starting compositions located very near to the α/β-Sialon phase border, as seen in Fig. 5a and b, but grains separated by a thin film also seem to be present, see Fig. 5a. In sample CCH16 (Fig. 5c and d), whose composition is close to the other end of Ca-α-Sialon phase region, a thin glass film with thickness about 0.9 nm is observed, but it is hard to estimate the dimension of glass phase at the triple-grain pockets. The observations seems to indicate that these samples contain only a small amount of grain boundary phase which in turn might

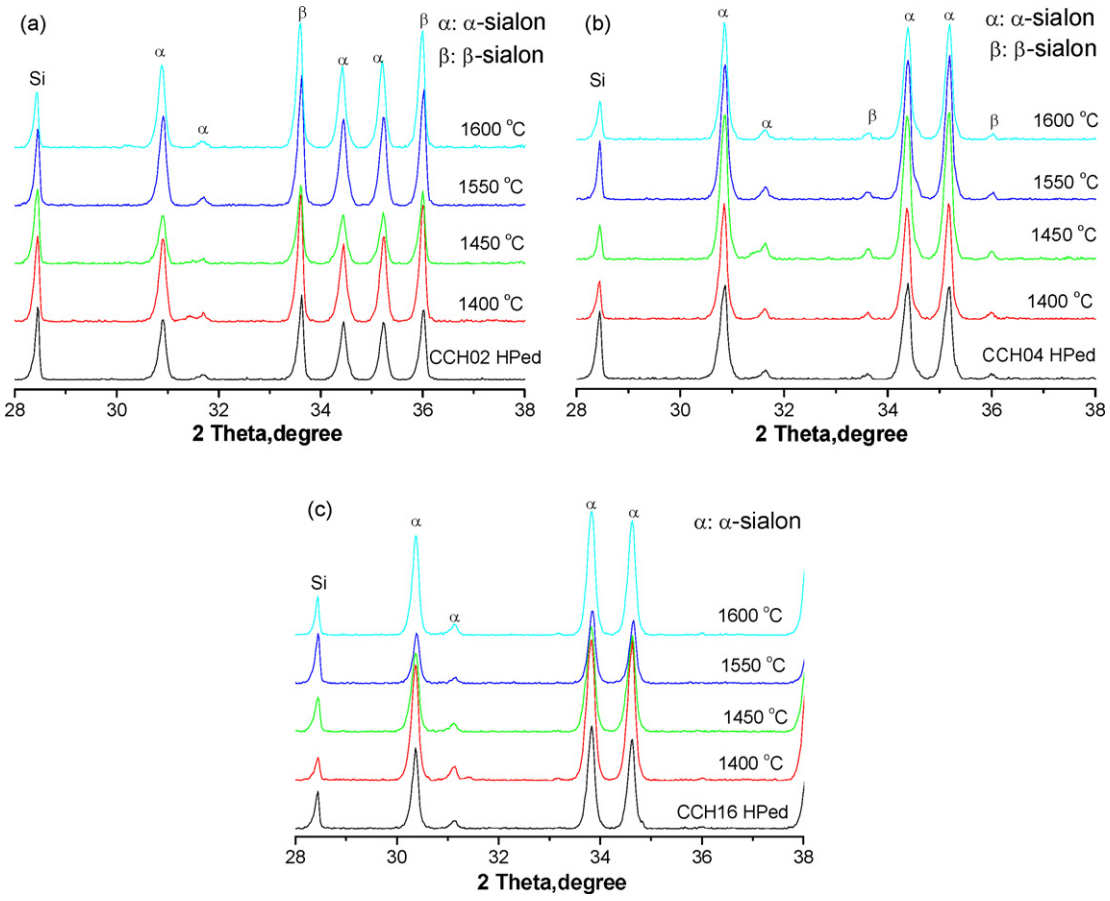

Fig. 4. X-ray powder diffraction analysis of samples CCH02 (an α/β-Sialon), CCH04 (an α-Sialon containing traces of α-Sialon) and CCH16 (an α-Sialon) post heat treated for 24 h at temperatures ranging from 1400 °C to 1600 °C for 24.

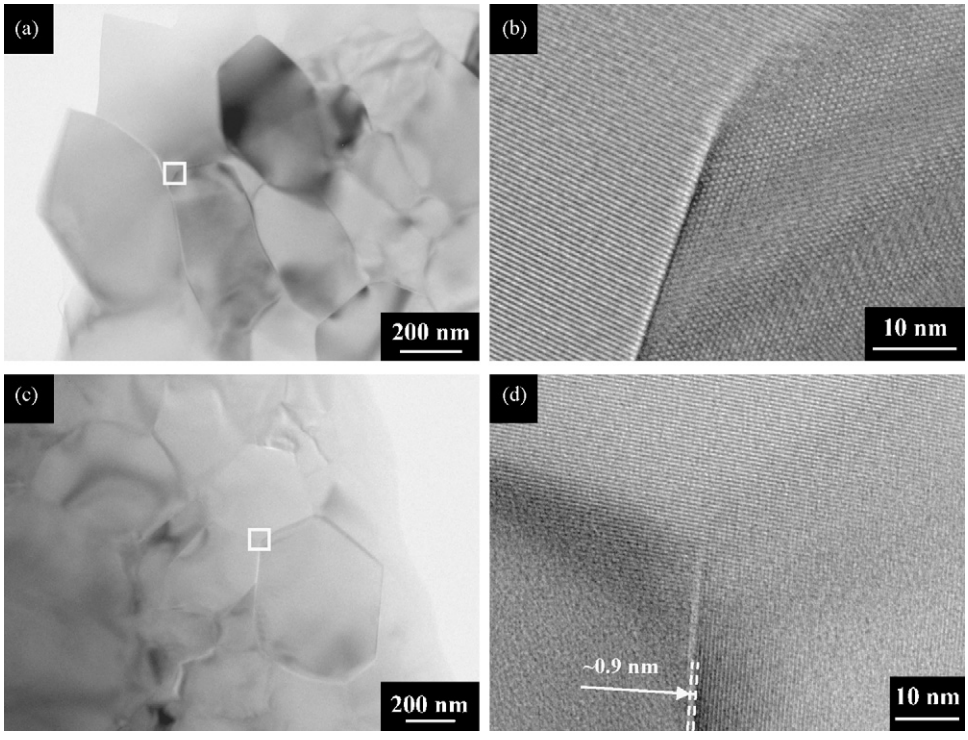

Fig. 5. TEM and corresponding HRTEM images for nitrogen-rich Ca-α-Sialons hot pressed at 1800 °C for 4 h: CCH04 (a) and (b); CCH16 (c) and (d).

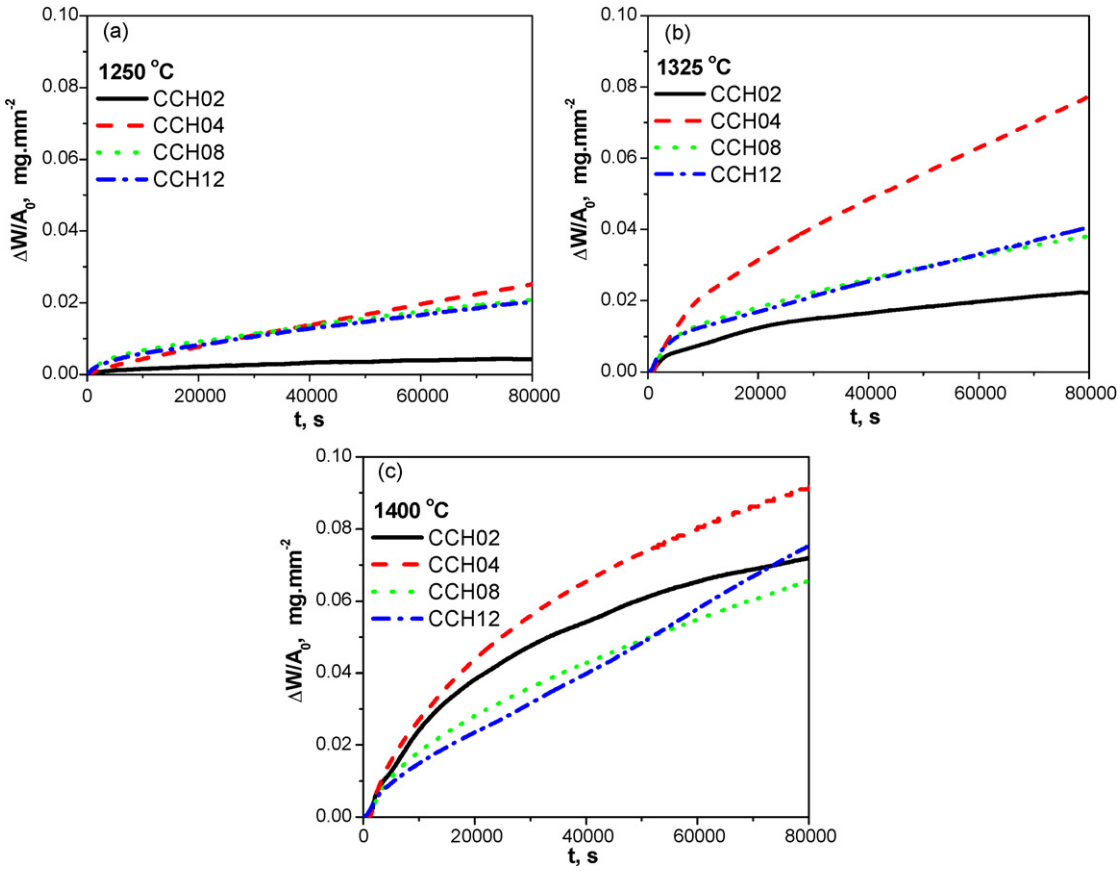

Fig. 6. Weight gains as a function of time of the nitrogen-rich Ca-α-Sialons oxidized at 1250 °C (a), 1325 °C (b) and 1400 °C (c) for 20 h in flowing oxygen.

explain the no α→β-Sialon transformation taking place in these samples.

3.5. Oxidation of nitrogen-rich Ca-α-Sialon

In principle, the nitrogen-rich α-Sialon compositions are thermally less stable in the presence of oxygen, i.e. more prone to be oxidized, than their oxygen-rich counterparts. Initially a thin oxygen rich layer is formed and as the oxidation proceeds, the thickness of the product layer increases, and the diffusion of the reactants and product gases through the product layer is retarded. The shape of the recorded oxidations curves at 1250 and 1325 °C (see Fig. 6) are generally speaking of the parabolic type while at 1400 °C they deviate from the parabolic type, seemingly a consequence of formation of bubbles in larger quantities, see below. At 1250 °C, the α/β-Sialon (CCH02) shows lower oxidation rates than those of the other samples that are phase pure α-Sialons (CCH08, CCH12) or contain traces of β-Sialon (CCH04). The latter compositions exhibit very similar oxidation rates. Higher oxidation rates are found at 1325 °C and the CCH02 sample exhibits the lowest degree of oxidation. The CCH04 composition exhibits the highest oxidation rate while the oxidation rates of CCH08 and CCH12 are almost the same. As mentioned above the oxidation curves recorded at 1400 °C deviate from the parabolic type and more pronounced so for the compositions CCH08 and CCH12 that exhibit almost linear oxidation rate curves.

The oxidation products, identified via their X-ray powder diffraction patterns, are listed in Table 2. Cristobalite (SiO_2) and wollastonite ($CaSiO_3$) are the main crystalline phases detected in the surface oxide scale. Very small amount of anorthite ($CaAl_2Si_2O_8$) phase is detected in samples oxidized at 1250 °C.

Cross-section SEM images reveal the microstructures of Sialons after oxidation. In the oxide scale, crystalline $CaSiO_3$ and SiO_2 phase are present in the oxide scale for all samples oxidized at lower temperatures, but in decreasing amount with increasing Ca content. A Ca–Si–Al–O glass is formed at all temperatures and the amount of crystalline phases in the oxide scale decreases with increasing Ca content. Based on SEM image observations and EDS analysis of the oxide scale, it seems that $CaSiO_3$ phase tends to be present on the top surface of the oxide scale, while SiO_2 phase is found on the surface of oxide scale obtained from low temperature oxidation, but more in the whole oxide scale obtained from high temperature oxidation. Fore example, in sample CCH02 more oxidation product $CaSiO_3$ is observed at 1250 °C, but better well shaped oxidation product SiO_2 at 1400 °C (see Fig. 7). The SiO_2 phase with a specific morphology is found to be crystallized from the liquid phase formed at temperatures above 1325 °C. And this has been further confirmed by EDS point analysis. When comparing SEM images (Fig. 8) of compositions CCH02, CCH04 and CCH08 oxidized at 1250 °C, a trend is found that the amount of crystalline phases in the oxide scale decreases with increase in Ca content, while glass formed has an opposite tendency.

Table 2
Phases in oxidation scales identified via their X-ray powder patterns.[a].

Sample	CCH02	CCH04	CCH08	CCH12
As sintered at 1800 °C	α-Sialon (62 mol/%) β-Sialon (38 mol/%)	α-Sialon (97 mol/%) β-Sialon (3 mol/%)	α-Sialon (100 mol/%)	α-Sialon (100 mol/%)
Oxidized at 1250 °C	SiO_2, s $CaSiO_3$, s $CaAl_2Si_2O_8$, w	SiO_2, s $CaSiO_3$, w $CaAl_2Si_2O_8$, w	SiO_2, s $CaSiO_3$, w $CaAl_2Si_2O_8$, vw	SiO_2, m $CaSiO_3$, w
Oxidized at 1325 °C	SiO_2, s $CaSiO_3$, m	SiO_2, s $CaSiO_3$, vw	SiO_2, w	SiO_2, w
Oxidized at 1400 °C	SiO_2, s $CaSiO_3$, w	SiO_2, s	SiO_2, vw	Amorphous

[a] Strength of reflections in XRPD pattern: s, strong; m, medium; w, weak; vw, very weak.

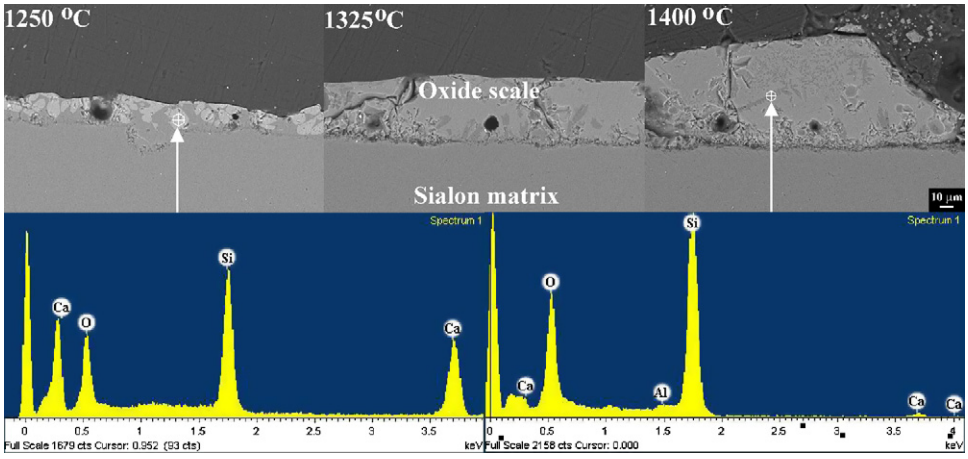

Fig. 7. Cross-section images of sample CCH02 oxidized at 1250 °C, 1325 °C and 1400 °C. Corresponding EDS analysis indicates the compositions of the crystalline phases formed within the oxide scale: $CaSiO_3$ phase at low temperature, but more SiO_2 phase at high temperature in which small amount of Ca, and Al is also detected from the surrounding glass.

An interface, typically containing bobbles formed due to the release of nitrogen in connection with the oxidation, is clearly visible and is located between the Sialon matrix and the outer part of the oxide scale (see Figs. 7–9). With increasing temperature and calcium content, both the amounts of glass phase and number of bubbles increase.

The oxidation of Ca-Sialon ceramics involves concurrently ongoing inward diffusion of oxygen and outward diffusion of metal cations and nitrogen products, resulting in compositional gradients. This is evident when EDS mapping technique is applied to the cross-section region obtained by ion-polishing techniques. As shown in Fig. 10, calcium and oxygen are enriched in the surface area, and gradually decrease inward, while silicon and nitrogen exhibit a positive elemental distribution, together with a homogenous distribution of aluminum over the whole area. The gradient distribution of elements

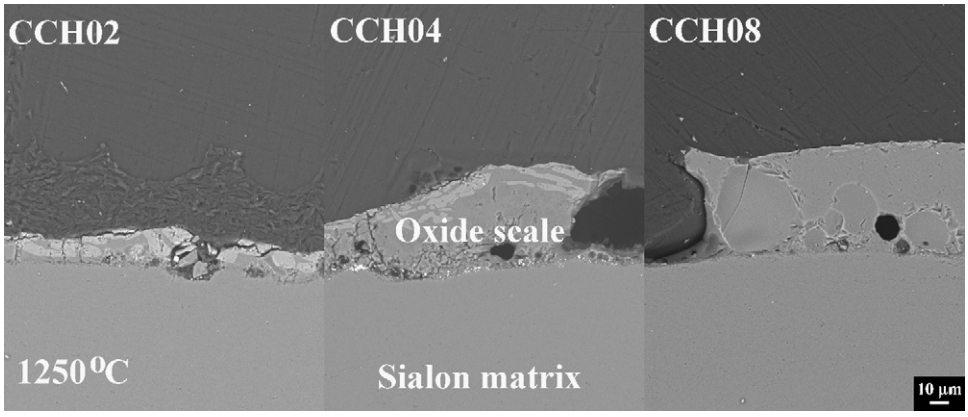

Fig. 8. Cross-section images of samples CCH02, CCH04 and CCH08 oxidized at 1250 °C.

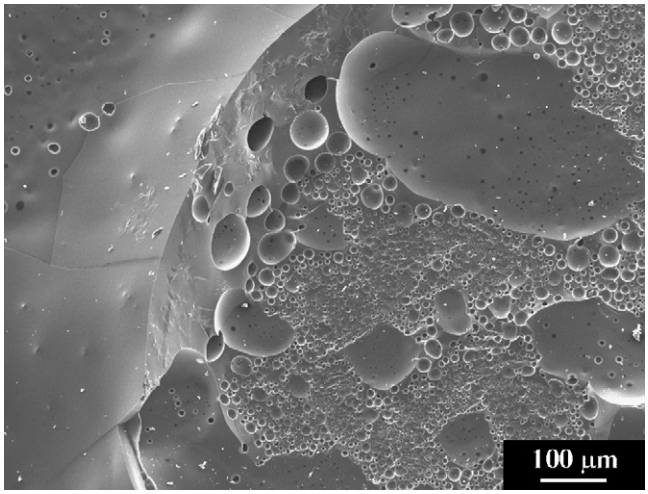

Fig. 9. An SEM image shows the formation of bubbles beneath the glass film in sample CCH08 oxidized at 1250 °C.

at the reaction region suggest that the diffusion of calcium and oxygen through the oxide layer and glass film is a rate controlling step in the oxidation of nitrogen-rich Ca-Sialon ceramics.

The formation sequence of these oxidation products, SiO_2, $CaSiO_3$ and $CaAl_2Si_2O_8$ for the nitrogen-rich Ca-α-Sialons is quite interesting but difficult to identify, since the oxidation is a dynamical process, involving concurrent diffusion of O, N, Ca, Si and Al through the oxide scale. It is assumed that: during the oxidation process, grain boundaries and grain boundary glass phase are usually the weak points to be first oxidized. According to EELS (electron energy loss spectra) analysis on the nitrogen-rich Ca-α-Sialons, it is found that the center of the α-Sialon grains is rich in Si, Al, N and almost oxygen free, but their relative contents go down towards the grain boundaries, which are rich in Ca and O. So it seems that the obtained α-Sialon grains have a core-shell structure. Consequently, during the oxidation process, outward diffusion of Ca and Si through the glass phase results in the formation and enrichment of $CaSiO_3$ phase at the top surface of the oxide scale, while inward diffusion of O results in the formation of SiO_2 phase on the inner side of the oxide scale (Fig. 7). From SEM (BSE mode) observation and EDS analysis, there is no observation of the $CaAl_2Si_2O_8$ phase, probably because the atomic numbers of Si and Al are very close, thus results in a low contrast in SEM images. In addition, Si and Al act as network-former in the oxynitride glasses, while Ca is an active network-modifier. The three elements, together with O and N,

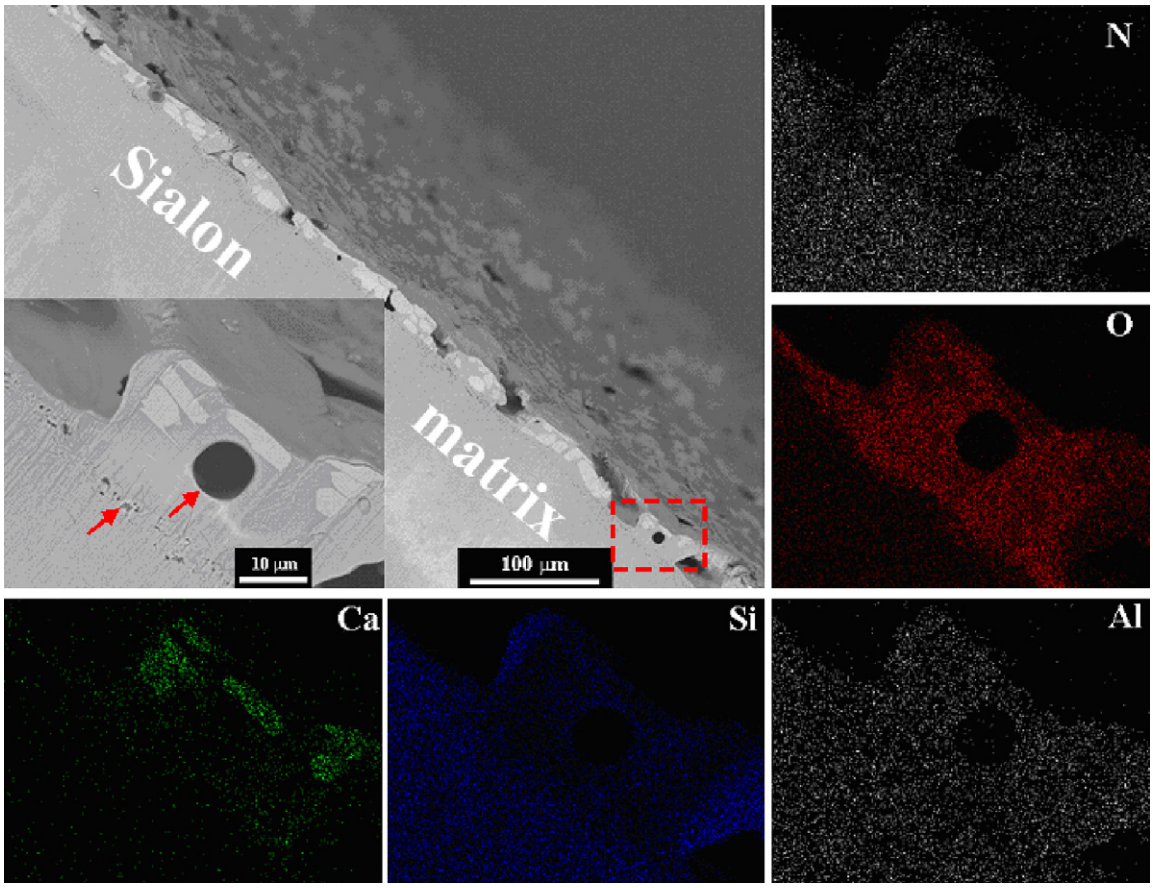

Fig. 10. EDS mapping analysis focused on cross-section region in sample CCH02 oxidized at 1250 °C. Note the depletion of calcium and bubbles at the interface and in the oxides scale (arrowed), but enrichment of calcium and oxygen at the surface.

EDS mapping analysis focused on cross-section region in sample CCH02 oxidized at 1250 °C. Note the depletion of calcium, and bubbles in the oxides scale (arrowed), but enrichment of calcium and oxygen at the surface.

tend to form a glass phase, which makes it more difficult to detect the $CaAl_2Si_2O_8$ phase in the oxide scale. This approximately accounts for the identification of $CaAl_2Si_2O_8$ phase mainly in the oxide scale obtained from the low temperature oxidation of α-Sialons with low Ca content, in which a much smaller amount of glass is formed after oxidation.

4. Conclusions

Nitrogen-rich Ca-α-Sialons have been prepared from appropriate mixtures of Si_3N_4, AlN and CaH_2, and the TG-study of these powder mixtures in nitrogen atmosphere showed that the decomposition of CaH_2 took place in the temperature region 200–300 °C and was followed by a significant nitridation within the temperature range 600–800 °C. The hot press study showed that α-Sialon phase was first observed at 1400 °C and monophasic Ca-α-Sialon ceramics was prepared at 1800 °C. Post heat treatment of the nitrogen-rich Ca-α-Sialons in the temperature range1400–1600 °C revealed that these Sialons are stable, i.e. no observation of α→β-Sialon transformation. The nitrogen-rich Ca-α-Sialons are less resistant to oxidation when compared to rear earth stabilized Sialons, while the mixed α/β-Sialon (low Ca content) shows better oxidation resistance than pure α-Sialon at low temperatures (1250–1325 °C). The low oxidation resistance of nitrogen-rich Ca-α-Sialons might be of major concern in connection with their potential applications such as cutting inserts, although they exhibit good combination of hardness and toughness. Anyhow, we are presently preparing nitrogen-rich, rear earth stabilized Sialons.

Acknowledgements

Special thanks to Daliang Zhang and Changhong Xiao of Structural Chemistry, Stockholm University for the TEM and HRTEM observations, and the ion-thinning operations, respectively. The authors thank Thomas Höche of Leibniz-Institut für Oberflächenmodifizierung for TEM specimen preparation and EELS analysis, the Swedish Research Council for financial support, and the Knut and Alice Wallenberg Foundation for the support of Electron Microscopy Center at Stockholm University.

References

1. Ekström, T. and Nygren, M., SIALON ceramics. *J. Am. Ceram. Soc.*, 1992, **75**, 259–276.
2. Cao, G. Z. and Metselaar, R., α'-Sialon ceramics: a review. *Chem. Mater.*, 1991, **3**, 242–252.
3. Cai, Y., Shen, Z., Grins, J. and Esmaeilzadeh, S., Self-reinforced nitrogen-rich calcium α-sialon ceramics. *J. Am. Ceram. Soc.*, 2007, **90**, 608–613.
4. Xie, R. J., Mitomo, M., Xu, F. F., Uheda, K. and Bando, Y., Preparation of Ca-α-sialon ceramics with compositions along the Si_3N_4–1/2Ca_3N_2:3AlN line. *Z. Metallkd.*, 2001, **92**, 931–936.
5. Cai, Y., Shen, Z., Höche, T., Grins, J. and Esmaeilzadeh, S., Super plastic deformation of nitrogen-rich Ca-α-Sialon ceramics. *Mater. Sci. Eng. A*, 2008, **475**, 81–86.
6. Wang, P. L., Zhang, C., Sun, W. Y. and Yan, D. S., Characteristics of Ca-α-sialon-phase formation, microstructure and mechanical properties. *J. Eur. Ceram. Soc.*, 1999, **19**, 553–560.
7. Tokoyoda, K., Hino, S., Ichikawa, T., Okamoto, K. and Fujii, H., Hydrogen desorption/absorption properties of Li–Ca–N–H system. *J. Alloys Compd.*, 2007, **439**, 337–341.
8. Xiong, Z., Wu, G., Hu, J. and Chen, P., Ternary imides for hydrogen storage. *Adv. Mater.*, 2004, **17**, 1522–1525.
9. Pinkerton, F. E. and Meyer, M. S., Reversible hydrogen storage in the lithium borohydride–calcium hydride coupled system. In *2008 APS March Meeting, Hydrogen Storage*, 2008.
10. Andreasen, A., *Hydrogen storage materials with focus on main group I–II elements*. Doctorial thesis, Technical University of Denmark, Lyngby, Denmark, 2005.
11. Rutten, J. W. T., Hintzen, H. T. and Metselaar, R., Phase formation of Ca-α-sialon sintering. *J. Eur. Ceram. Soc.*, 1996, **16**, 995–999.
12. Hewett, C. L., Cheng, Y.-B., Muddle, B. C. and Trigg, M. B., Thermal stability of calcium α-sialon ceramics. *J. Eur. Ceram. Soc.*, 1998, **18**, 417–427.
13. Mandal, H. and Thompson, D. P., α→β sialon transformation in calcium-containing α-SiAlON ceramics. *J. Eur. Ceram. Soc.*, 1999, **19**, 543–552.
14. Seeber, A. J. and Cheng, Y.-B., Thermal stability of mixed-cation α-sialon ceramics. *Mater. Sci. Eng. A*, 2003, **339**, 115–123.
15. Rosenflanz, A. and Chen, I.-W., Kinetics of phase transformations in SiAlON ceramics. I. Effects of cation size, composition and temperature. *J. Eur. Ceram. Soc.*, 1999, **19**, 2325–2335.
16. Shen, Z., Ekström, T. and Nygren, M., Temperature stability of samarium-doped α-SiAlON ceramics. *J. Eur. Ceram. Soc.*, 1996, **16**, 43–54.
17. Carman, A., Pereloma, E. and Cheng, Y.-B., Reversible α'↔β' transformation in preferentially oriented sialon ceramics. *J. Eur. Ceram. Soc.*, 2006, **26**, 1337–1349.
18. Camuscu, H., Thompson, D. P. and Mandal, H., Effect of starting composition, type or rare earth sintering additive and amount of liquid phase on α↔β SiAlON transformation. *J. Eur. Ceram. Soc.*, 1997, **17**, 599–613.